



7N-02  
144263  
368

# TECHNICAL NOTE

## D-37

EFFECTS OF BODY AND FIN DEFLECTIONS ON THE AERODYNAMIC  
CHARACTERISTICS IN PITCH OF A 0.065-SCALE MODEL  
OF A FOUR-STAGE ROCKET CONFIGURATION AT  
MACH NUMBERS OF 1.41 AND 1.82

By Ross B. Robinson

Langley Research Center  
Langley Field, Va.

NATIONAL AERONAUTICS AND SPACE ADMINISTRATION  
WASHINGTON

September 1959

(NASA-TN-D-37) EFFECTS OF BODY AND FIN  
DEFLECTIONS ON THE AERODYNAMIC  
CHARACTERISTICS IN PITCH OF A .065-SCALE  
MODEL OF A FOUR-STAGE ROCKET CONFIGURATION  
AT MACH NUMBERS OF 1.41 AND 1.82 (NASA.

N89-70757

Unclas  
00/02 0194263

## NATIONAL AERONAUTICS AND SPACE ADMINISTRATION

## TECHNICAL NOTE D-37

## EFFECTS OF BODY AND FIN DEFLECTIONS ON THE AERODYNAMIC

## CHARACTERISTICS IN PITCH OF A 0.065-SCALE MODEL

## OF A FOUR-STAGE ROCKET CONFIGURATION AT

## MACH NUMBERS OF 1.41 AND 1.82

By Ross B. Robinson

## SUMMARY

An investigation of the effects of body and fin deflections on the aerodynamic characteristics in pitch of a 0.065-scale model of a four-stage rocket configuration at Mach numbers of 1.41 and 1.82 has been made in the Langley 4- by 4-foot supersonic pressure tunnel. Provisions were made for deflecting each stage with respect to the next rearward stage. Cruciform fins were mounted on the first three stages. The fins on the first and second stages were always alined, whereas the fins on the third stage were tested both alined and indexed  $45^\circ$  with respect to the first- and second-stage fins.

The results indicate that significant bending moments at the various stage junctures and appreciable attitude changes of the complete configuration could be caused by relatively small amounts of body deflection. For angles of attack up to about  $4^\circ$  the variation of pitching-moment coefficient with angle of attack was linear for both the indexed- and alined-fin configurations. In the angle-of-attack range from about  $4^\circ$  to  $8^\circ$ , a region of increased stability was indicated for the arrangement with the indexed fins. With the fins alined, the stability was increased in the low angle-of-attack range. Differential deflection of the second- or third-stage fins produced negligible rolling moments for both the alined- and the indexed-fin configurations.

## INTRODUCTION

An investigation has been made of the aerodynamic characteristics in pitch of a 0.065-scale model of a research vehicle at Mach numbers of 1.41 and 1.82. The model simulated a complete four-stage rocket configuration and consisted of three booster rocket motors (an Honest John, a Nike, and an X-7) and a velocity package; the configuration was proposed by the Langley Pilotless Aircraft Research Division for reentry physics research. The purpose of this investigation was to determine the effects of body deflection, differential fin deflection, and fin alignment on the aerodynamic characteristics in pitch of the model.

This report presents six-component force and moment data for an angle-of-attack range of about  $-4^{\circ}$  to  $10^{\circ}$  at  $0^{\circ}$  sideslip.

## SYMBOLS

The results are referred to the body-axis system, with the moment reference point at a longitudinal station corresponding to 83.6 percent of the body length.

$C_N$	normal-force coefficient, $F_N/qS$
$C_A$	axial-force coefficient, $F_A/qS$
$C_Y$	side-force coefficient, $F_Y/qS$
$C_m$	pitching-moment coefficient, $M_Y/qSd$
$C_l$	rolling-moment coefficient, $M_X/qSd$
$C_n$	yawing-moment coefficient, $M_Z/qSd$
$F_N$	normal force
$F_A$	axial force
$F_Y$	side force
$M_Y$	pitching moment, moment about Y-axis
$M_X$	rolling moment, moment about X-axis
$M_Z$	yawing moment, moment about Z-axis

d	maximum body diameter, 1.65 in.
M	free-stream Mach number
q	free-stream dynamic pressure
S	maximum cross-sectional area of model, 2.138 sq in.
$\alpha$	angle of attack of stage 1 center line, deg
$\delta_B$	body deflection, relative to next rearward stage (pitch plane only), positive nose up, deg
$\delta_f$	fin deflection, deg

### MODELS AND APPARATUS

Details of the model are shown in figure 1 and the geometric characteristics are presented in table I and figure 2. Coordinates for the body are presented in table II. Photographs of the model are shown in figure 3.

The body was composed of four sections or stages having circular cross sections (fig. 1). The diameter of the first stage was enlarged about 3 percent to accommodate the balance. Provision was made to permit the deflection of each stage with respect to the next rearward stage. Deflections to  $1^\circ$  were obtained for stages 2 and 3 and to  $1/2^\circ$  for stage 4.

Cruciform fins were mounted on stages 1, 2, and 3 of the model. The fins on stage 1 were welded in place at approximately  $0^\circ$  deflection. Two fins on stage 2 and two fins on stage 3 could be deflected to provide roll control. The fins of stages 1 and 2 were always aligned, whereas those of stage 3 could be aligned or indexed  $45^\circ$  with respect to the others. Most of the tests were made with the indexed-fin configuration. A summary of the measured fin deflections is given in figure 2.

Forces and moments were obtained by means of an internal strain-gage balance. Base pressures were measured by four tubes placed just inside the base of the model.

### TESTS, CORRECTIONS, AND ACCURACY

The tests were made at Mach numbers of 1.41 and 1.82 for Reynolds numbers per foot of  $2.92 \times 10^6$  and  $2.62 \times 10^6$ , respectively. The



stagnation temperature for both tests was  $110^{\circ}$  F and the stagnation pressure was 1,440 lb/sq ft. The stagnation dewpoint was maintained sufficiently low (less than  $-25^{\circ}$  F) so that no condensation effects were encountered in the test section. Tests were made for an angle-of-attack range of about  $-4^{\circ}$  to about  $10^{\circ}$  at an angle of sideslip of  $0^{\circ}$ . The angles of attack and sideslip were corrected for the deflection of the balance and sting under load. The base pressure was measured, and the chord force was adjusted to a base pressure equal to free-stream static pressure.

The estimated precision of the individually measured quantities including repeatability, zero shifts, and balance calibration is as follows:

	M = 1.41	M = 1.82
$C_N$ . . . . .	$\pm 0.045$	$\pm 0.050$
$C_A$ . . . . .	$\pm 0.006$	$\pm 0.006$
$C_m$ . . . . .	$\pm 0.047$	$\pm 0.048$
$C_L$ . . . . .	$\pm 0.030$	$\pm 0.034$
$C_N$ . . . . .	$\pm 0.017$	$\pm 0.019$
$C_Y$ . . . . .	$\pm 0.030$	$\pm 0.033$
$\alpha$ , deg . . . . .	$\pm 0.1$	$\pm 0.1$
$\delta_f$ , deg . . . . .	$\pm 0.1$	$\pm 0.1$
$\delta_B$ , deg . . . . .	$\pm 0.1$	$\pm 0.1$
M . . . . .	$\pm 0.01$	$\pm 0.015$

## PRESENTATION OF RESULTS

The results are presented in the following figures:

	Figure
Effects of individual deflection of various stages	
at M = 1.41 . . . . .	4
Effects of combined deflections of various stages	
at M = 1.41 . . . . .	5
Effects of third-stage-fin alinement at M = 1.41 . . . . .	6
Effects of differential fin deflection, third-stage fins	
indexed, at M = 1.41 . . . . .	7
Effect of differential fin deflection, third-stage fins	
in line, at M = 1.41 . . . . .	8

## Figure

Effects of individual deflection of various stages	
at $M = 1.82$ . . . . .	9
Effects of combined deflections of various stages	
at $M = 1.82$ . . . . .	10
Effects of third-stage-fin alinement at $M = 1.82$ . . . . .	11
Effects of differential fin deflection, third-stage	
fins indexed, at $M = 1.82$ . . . . .	12
Effects of differential fin deflection, third-stage fins	
in line, at $M = 1.82$ . . . . .	13

## SUMMARY OF RESULTS

The majority of the tests were made with the fins of stage 3 indexed  $45^\circ$  with respect to the fins of stages 1 and 2. (See figs. 1 and 3.) The effects of body deflections were obtained with approximately  $0^\circ$  deflection of all fins, and the effects of fin deflections were measured for  $0^\circ$  deflections of the various stages comprising the body.

Deflection of the finned stages 2 and 3 individually (figs. 4 and 9) or in combination (figs. 5 and 10) produced appreciable increments in pitching-moment coefficient at both Mach numbers, whereas the effects of nose deflection (stage 4) were small. The moment increments resulting from combined deflections of stages 2 and 3 were approximately linear with deflection angle. These results indicate the possibilities of significant bending moments at the various stage junctures and also indicate that significant attitude changes of the complete configuration could be caused by relatively small amounts of body deflection.

For all the configurations tested the variation of  $C_m$  with  $\alpha$  was linear for angles of attack to about  $4^\circ$  at both Mach numbers. In the angle-of-attack range from about  $4^\circ$  to  $8^\circ$  a region of increased stability particularly at  $M = 1.41$  (figs. 4 and 9) was indicated by the pitching-moment coefficients of the indexed-third-stage arrangement. This region of increased stability probably results from a reduction in the lift of the second-stage fins as they pass through the wake of the third-stage fins in the angle-of-attack range from about  $4^\circ$  to  $8^\circ$ . These wake effects are smaller at  $M = 1.82$  because of the reduced lift-curve slope of the fins at the higher Mach number.

With the fins alined (flagged symbols in figs. 6 and 11), the second-stage fins are in the wake from the third-stage fins near  $0^\circ$  angle of attack and thus the stability for this arrangement is increased in the low angle-of-attack range. The variation of  $C_m$  with  $\alpha$  for the

alined-fin model is more linear through the entire  $\alpha$  range than it is for the indexed-fin arrangement.

Differential deflections of the third-stage fins are to be incorporated into the missile to provide spin stabilization for the third and fourth stages. Since differential deflection of these fins produced negligible rolling moments for the complete configuration having either indexed or alined fins (figs. 7, 8, 12, and 13), no opposite deflection of the fins on stage 2 should be necessary. The large fins on stage 1 appear to counteract the rolling moments produced by the deflection of either or both sets of forward surfaces.

The small negative values of  $C_n$  and  $C_y$  obtained at the higher angles of attack for both the indexed- and alined-fin configurations probably result from asymmetries in the model (figs. 6 and 11). Deflections of the body (figs. 5 and 10) or of the fins (figs. 7 and 12) produced somewhat larger negative values of  $C_n$  and  $C_y$ .

Langley Research Center,  
National Aeronautics and Space Administration,  
Langley Field, Va., April 16, 1959.

TABLE I.- GEOMETRIC CHARACTERISTICS OF MODEL

	Stage 4	Stage 3	Stage 2	Stage 1
<b>Body:</b>				
Length, in. . . . .	8.27	12.40	9.09	13.23
Diameter, in. . . . .	0.99	0.99	1.08	1.65
Cross-sectional area, sq in. . . . .	0.770	0.770	0.916	2.138
Center-of-gravity location, percent of model length . . . . .				0.836
Diameter of wing-body juncture, in. . . . .	0.99		1.18	1.65
<b>Fins:</b>				
Area (exposed), per pair, sq in. . . . .		2.454	3.102	9.362
Span (exposed), in. . . . .		2.36	2.82	5.26
Aspect ratio (exposed) . . . . .		2.27	2.56	2.96
Root chord, in. . . . .		1.41	1.53	2.97
Tip chord, in. . . . .		0.68	0.67	0.59
Taper ratio . . . . .		0.482	0.438	0.199
Thickness, in. . . . .		0.059	0.055	0.094

TABLE II.- BODY COORDINATES

Body station, in.	Diameter, in.	Remarks
0	0	Spherical nose, radius 0.177 in.
.177	.354	
.901	.557	
7.212	.987	
8.270	.987	End of fourth stage
20.670	.987	End of third stage
20.780	1.080	Transition to second stage
27.480	1.080	Transition to fin section
27.800	1.180	End of transition
29.760	1.180	End of second stage
30.310	1.650	Transition to first stage
42.990	1.650	End of first stage



Figure 1.- Drawing of model of four-stage rocket configuration. All dimensions are in inches.

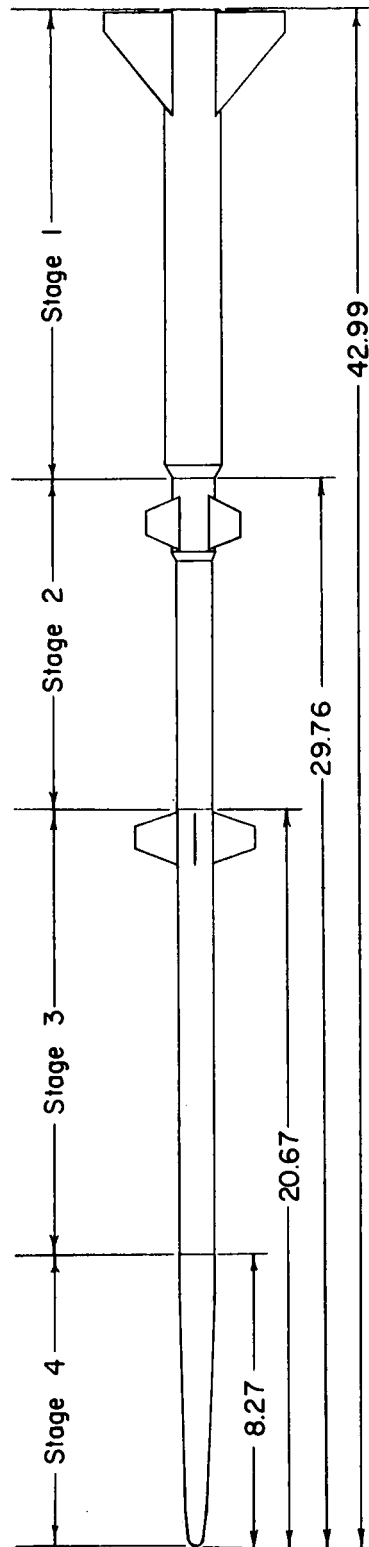
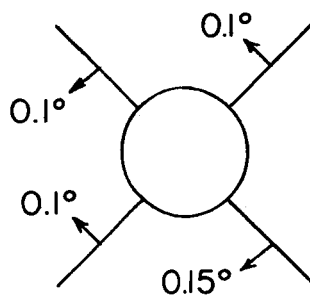
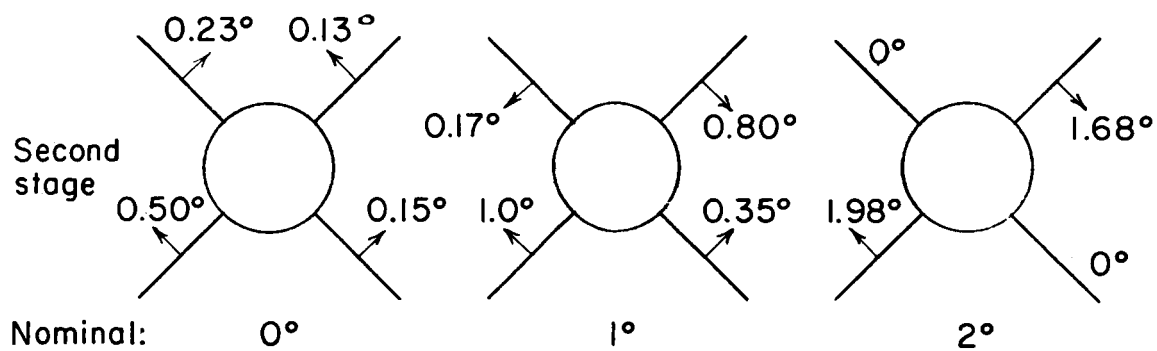


Figure 1.- Concluded.

First  
stage



Second  
stage



Third  
stage

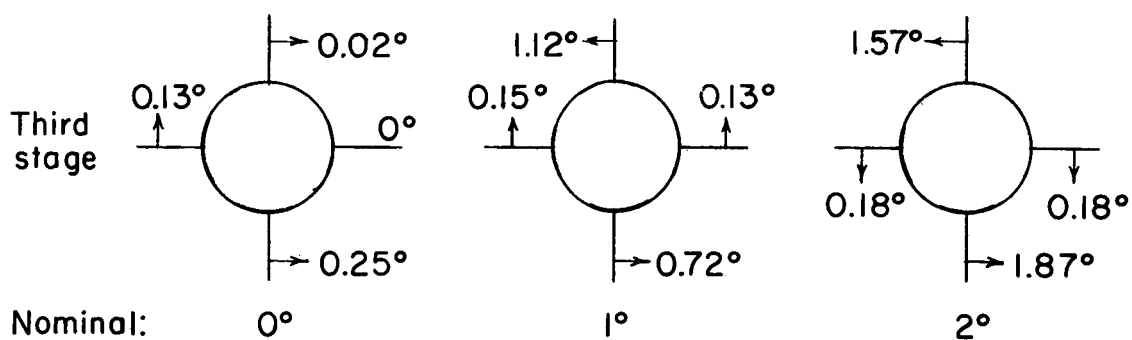
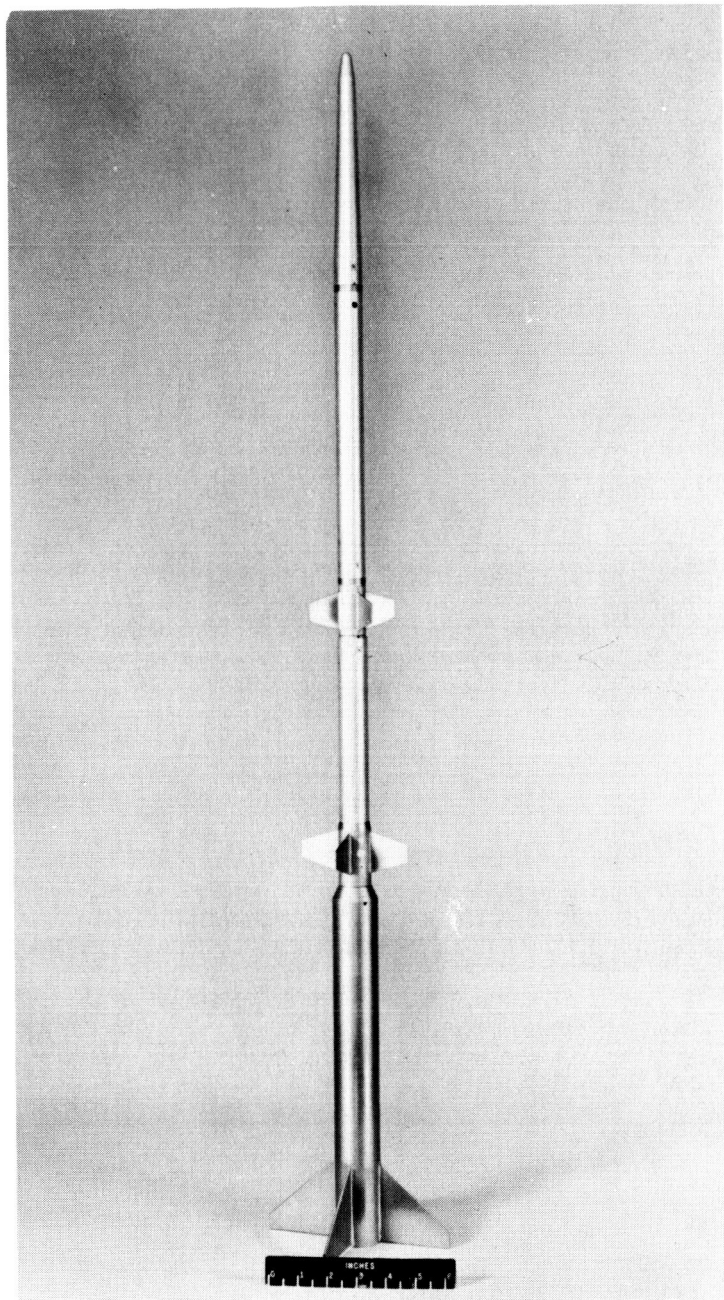


Figure 2.- Angular deflections of fin leading edge as viewed from rear.

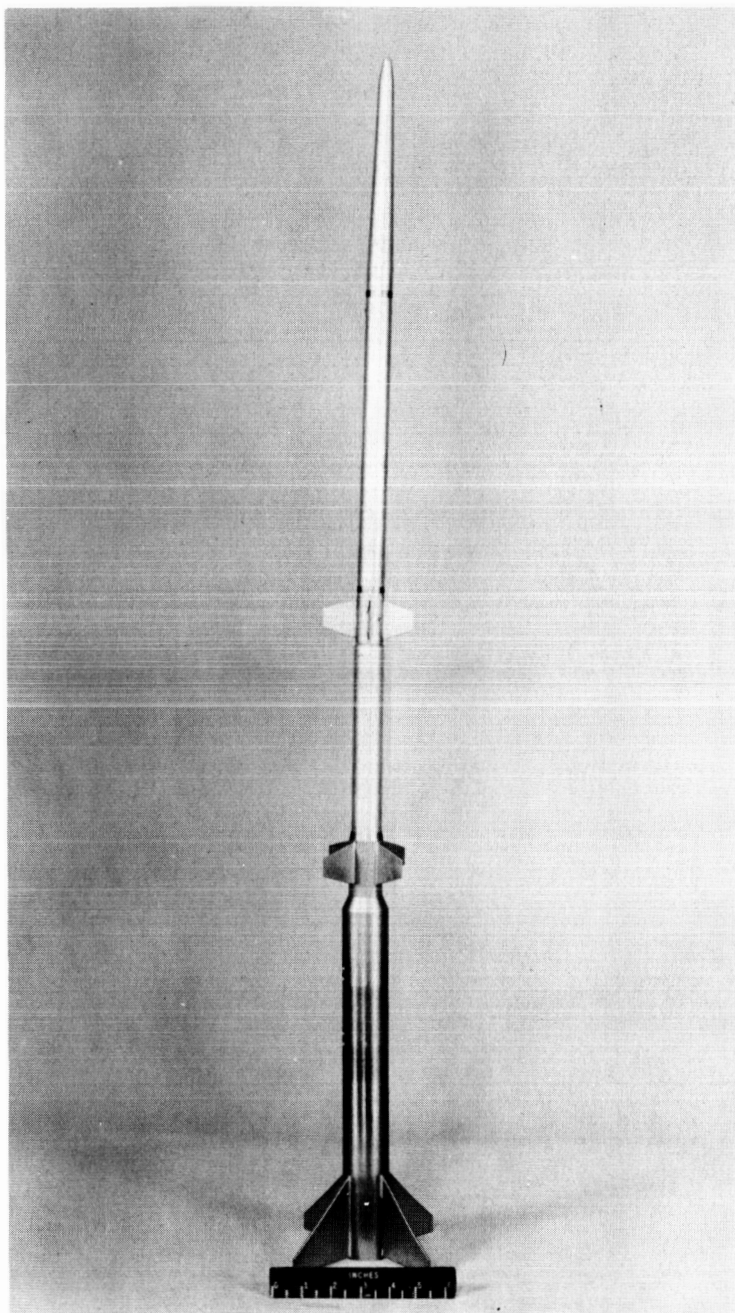




(a) Body undeflected.

L-58-3679

Figure 3.- Photographs of model of four-stage rocket configuration.



(b) Body deflected.

L-58-3678

Figure 3.- Concluded.

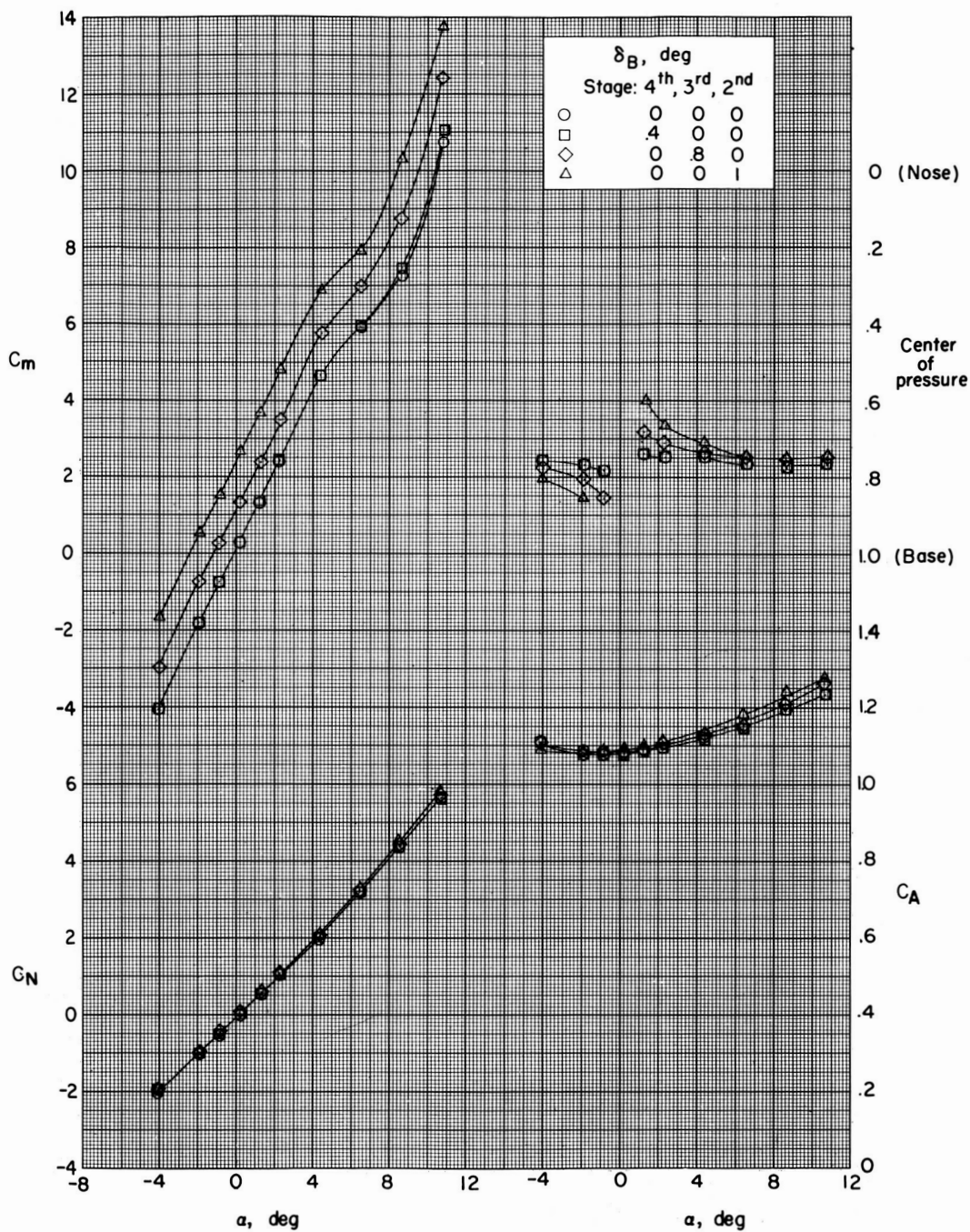


Figure 4.- Effects of individual deflection of various stages of four-stage rocket model. Third-stage fins indexed;  $M = 1.41$ .

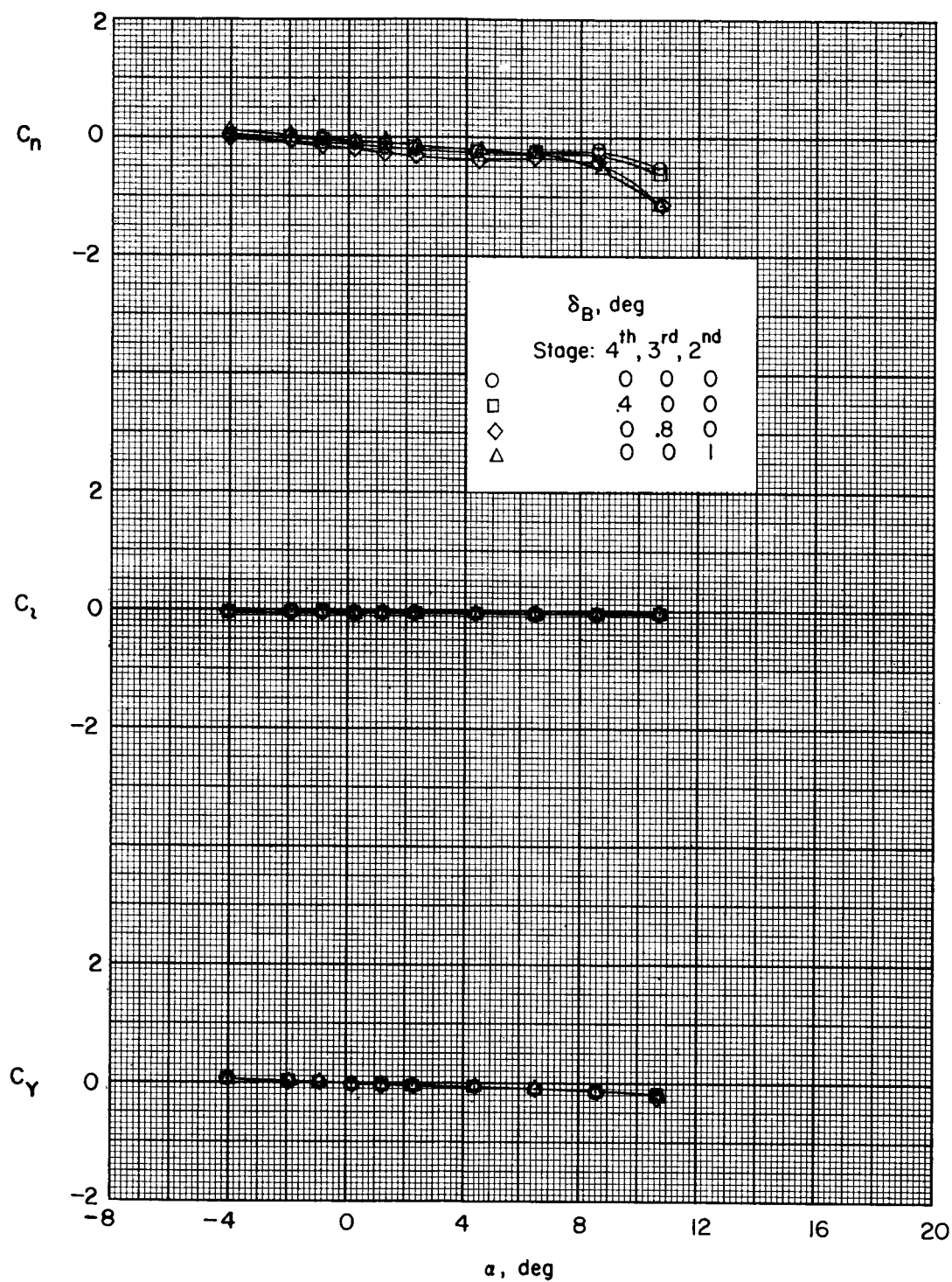


Figure 4.- Concluded.

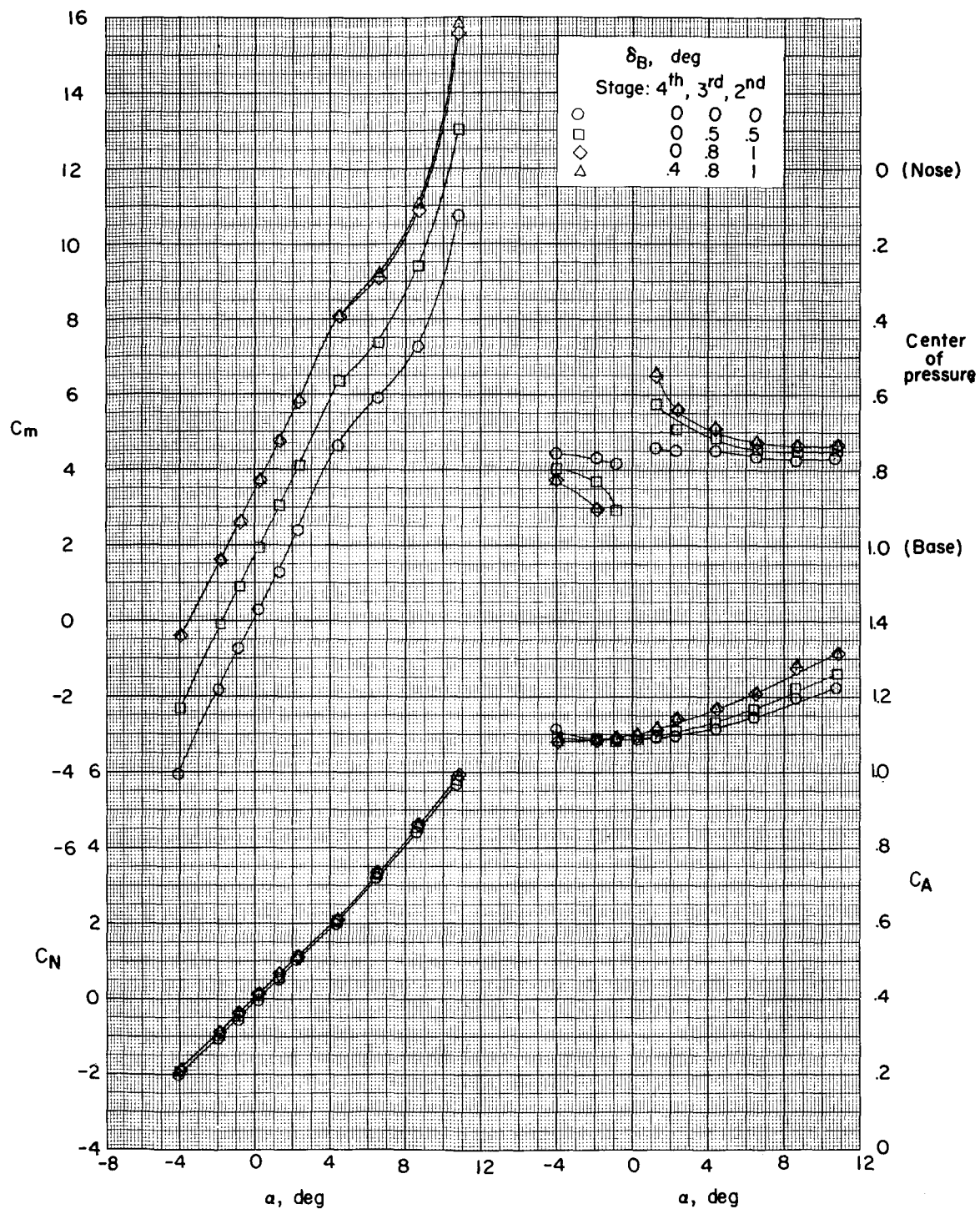


Figure 5.- Effects of combined deflections of various stages of four-stage rocket model. Third-stage fins indexed;  $M = 1.41$ .



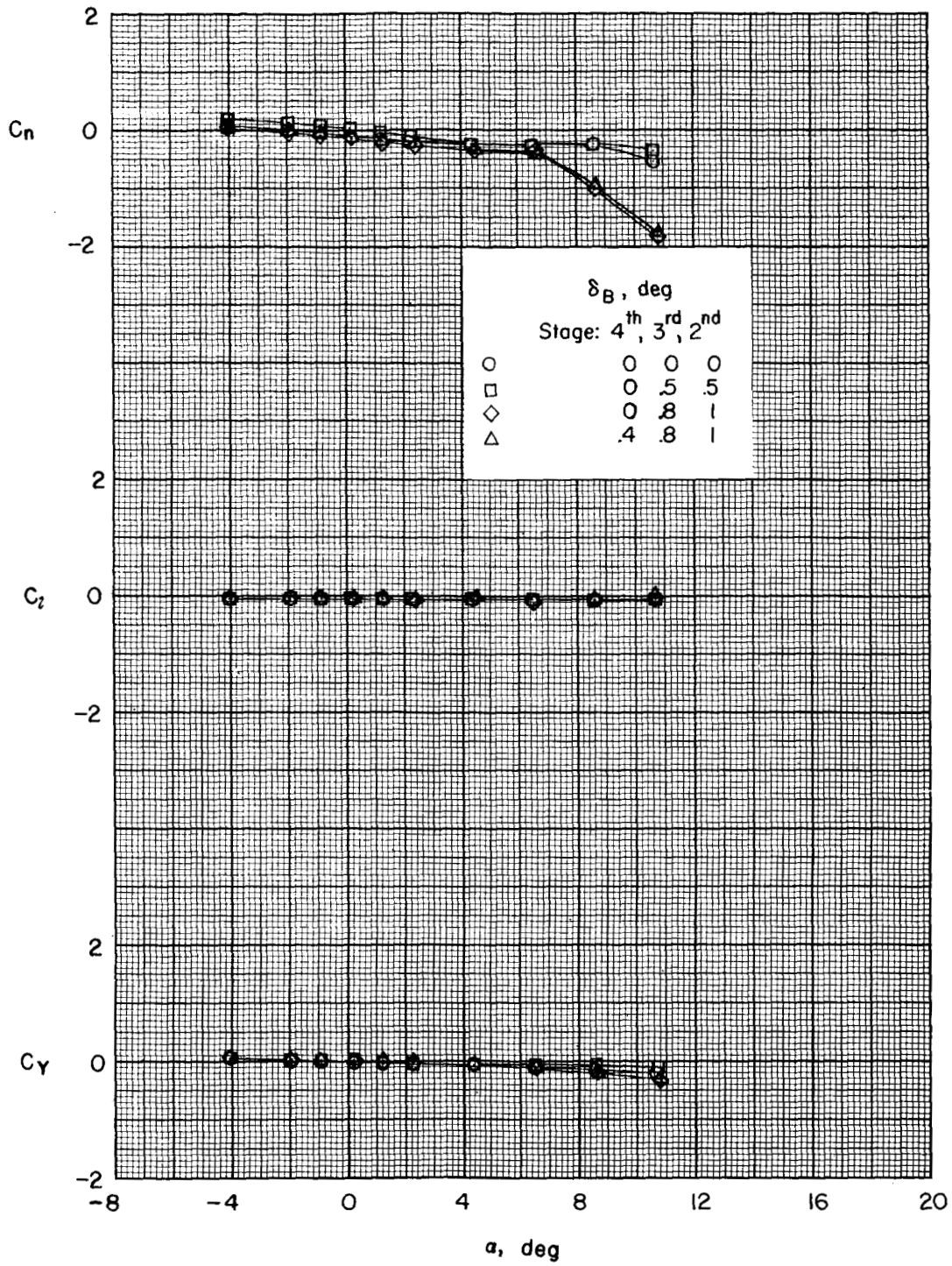


Figure 5.- Concluded.

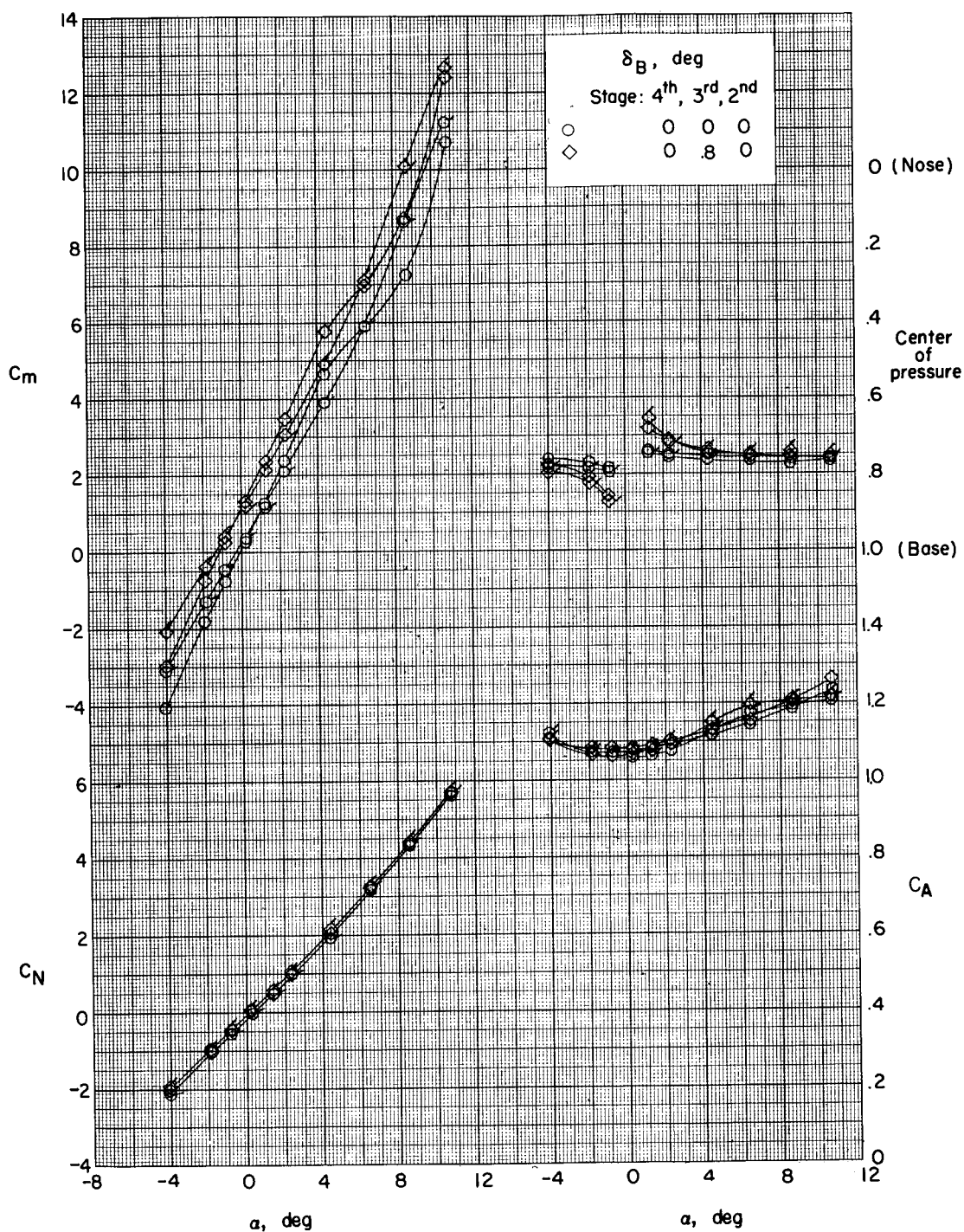


Figure 6.- Effects of third-stage-fin alignment. Plain symbols indicate indexed fins; flagged symbols indicate aligned fins;  $M = 1.41$ .

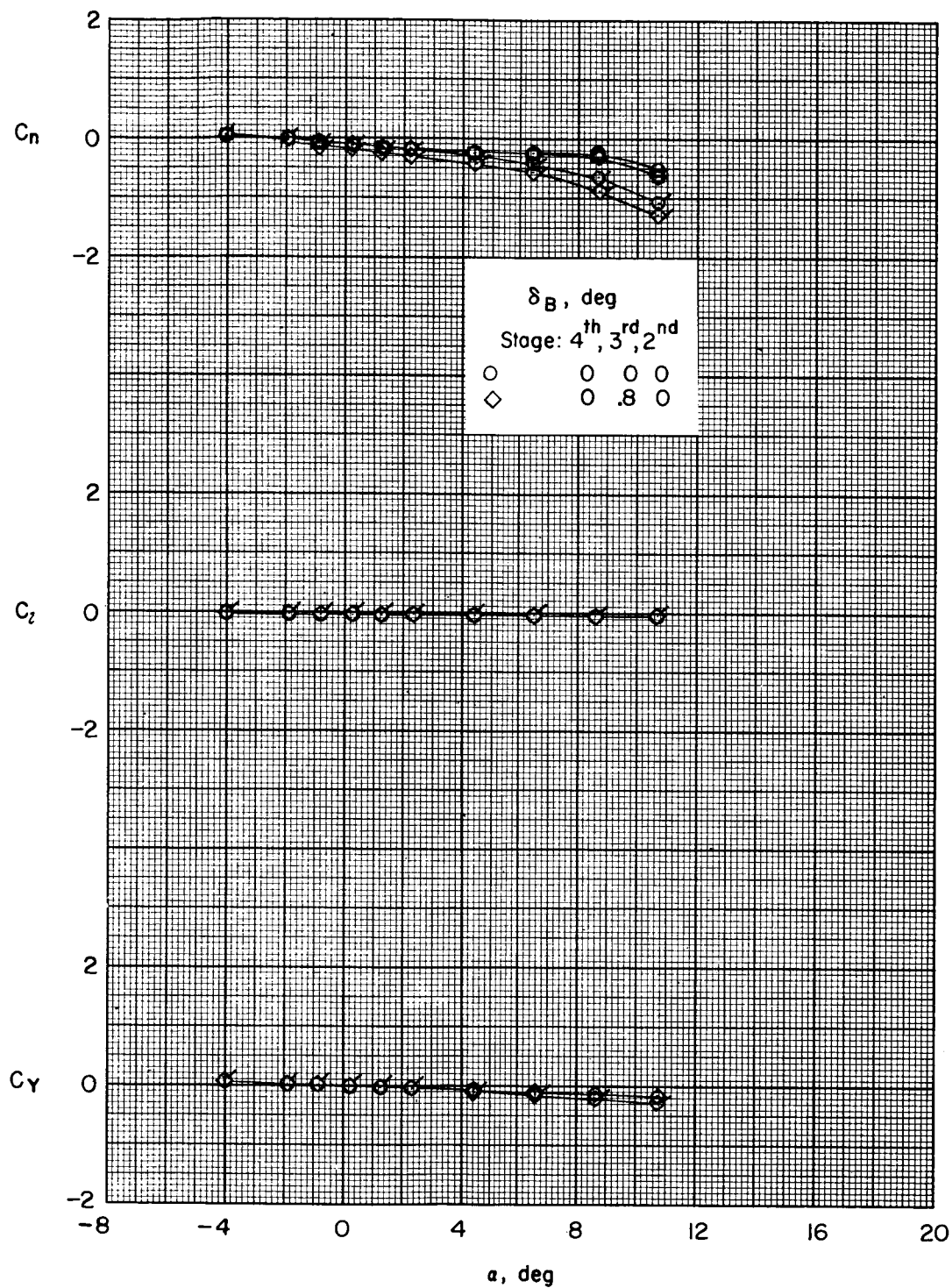


Figure 6.- Concluded.



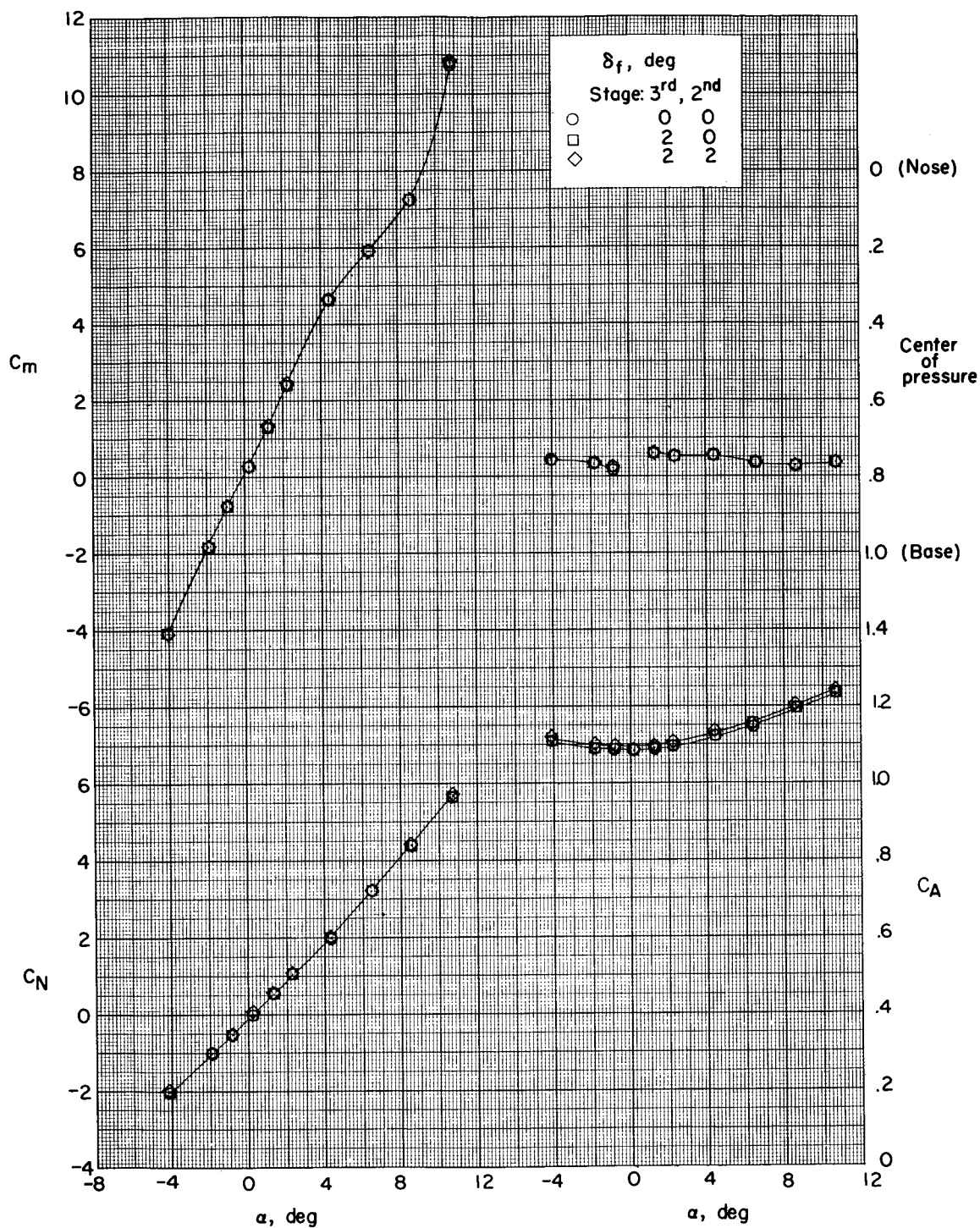


Figure 7.- Effects of differential fin deflection. Body deflection,  $0^\circ$ ; third-stage fins indexed;  $M = 1.41$ .

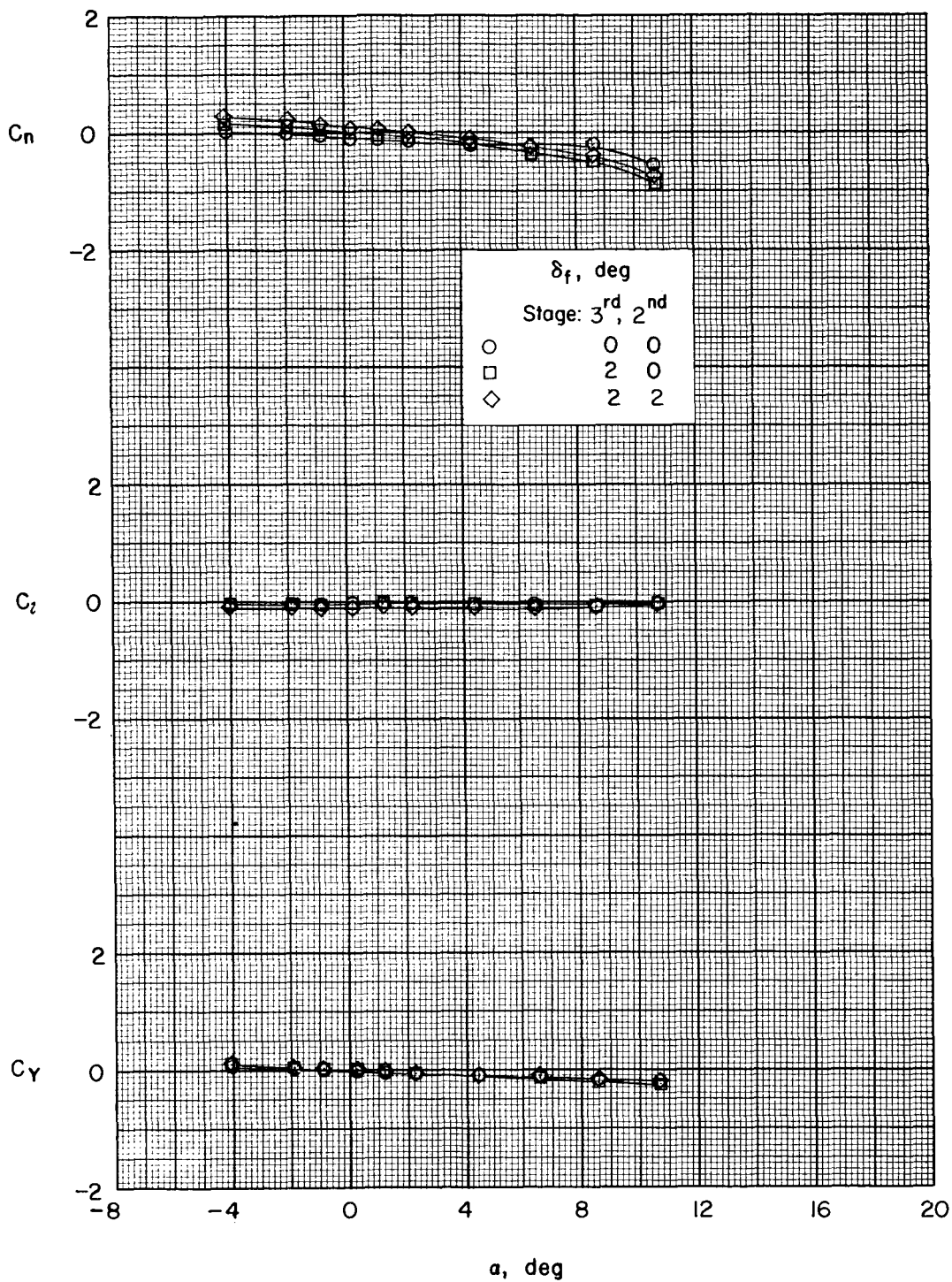


Figure 7.- Concluded.

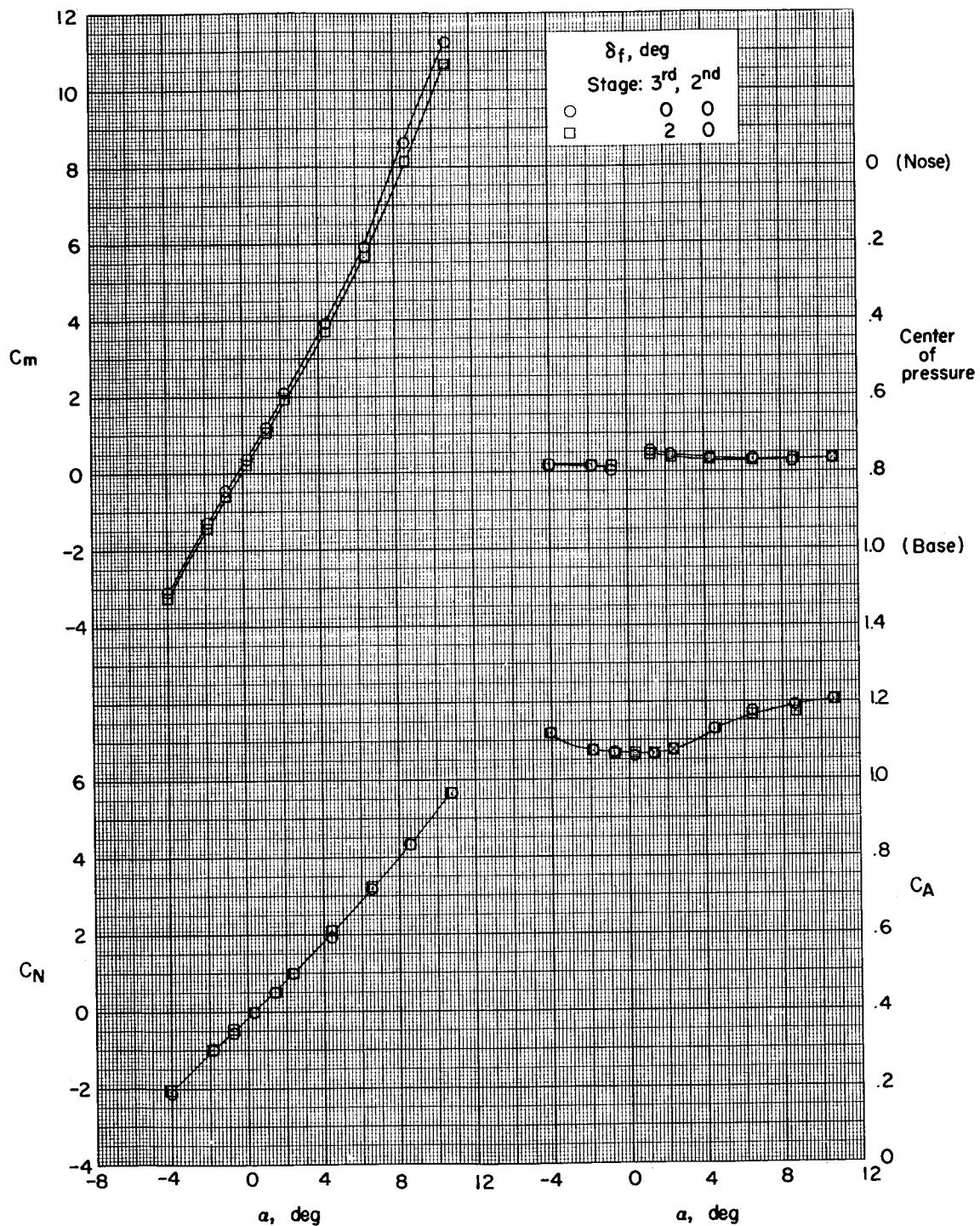


Figure 8.- Effects of differential fin deflection. Body deflection,  $0^\circ$ ; third-stage fins aligned;  $M = 1.41$ .

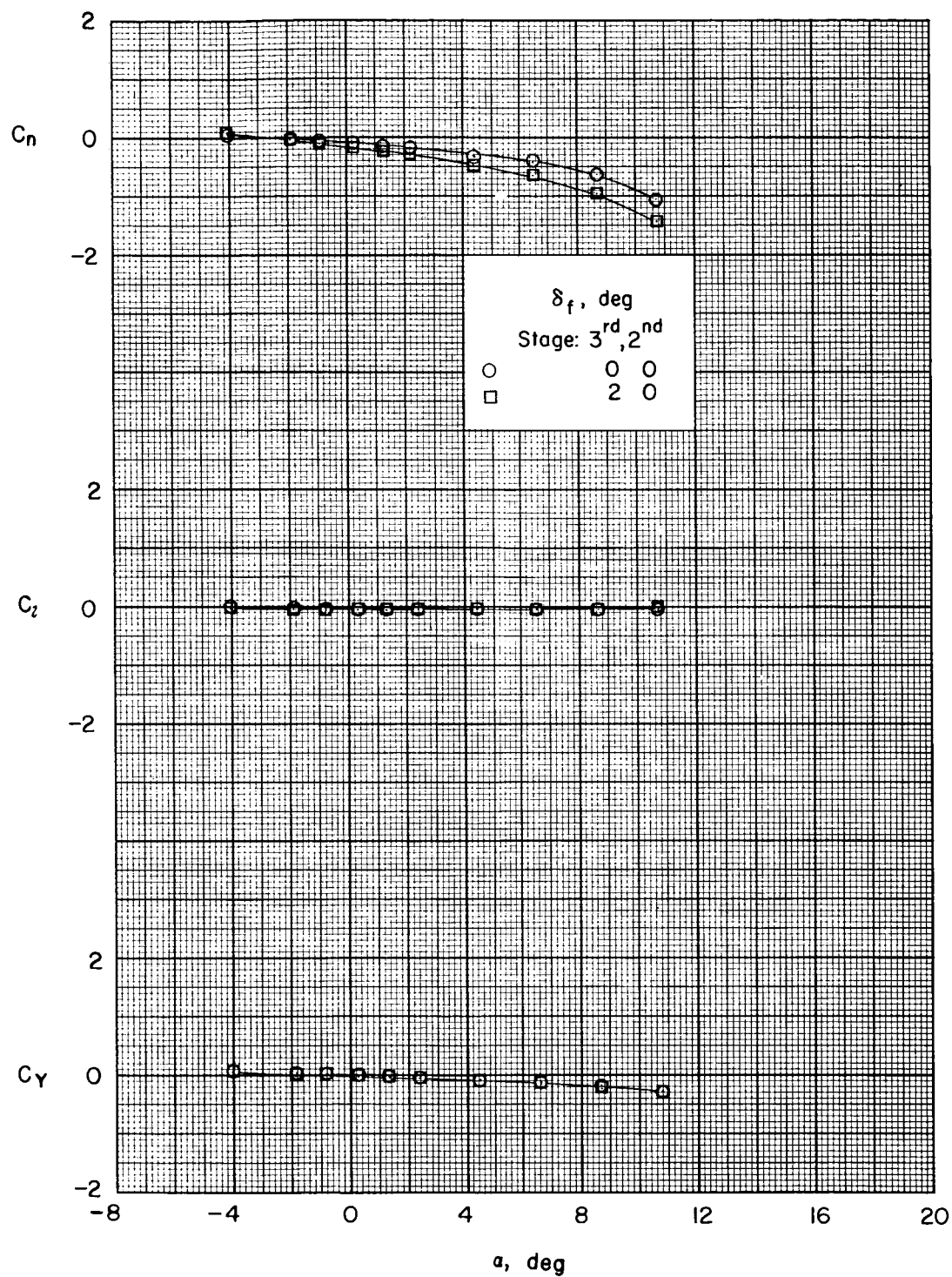


Figure 8.- Concluded.

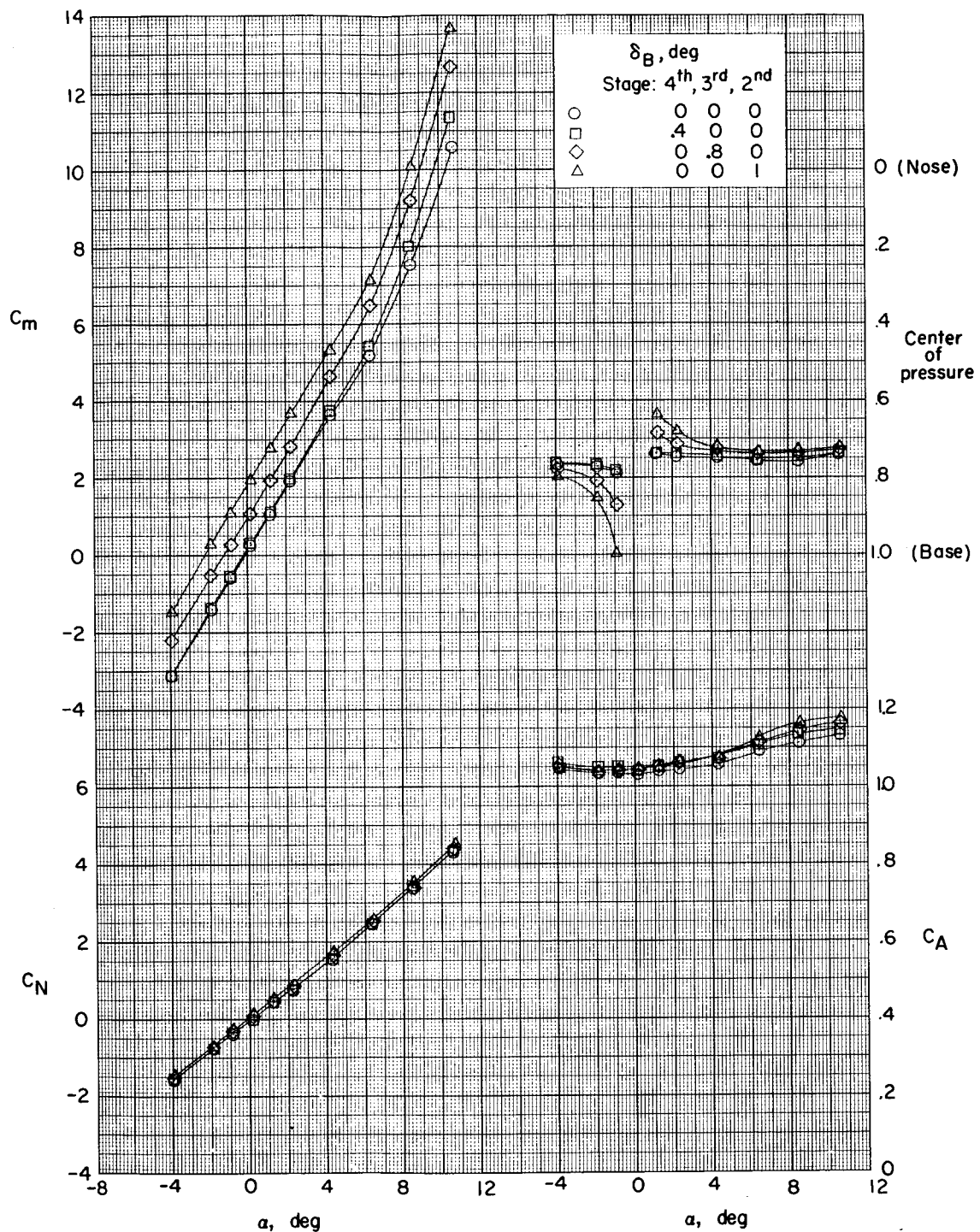


Figure 9.- Effects of individual deflection of various stages of four-stage rocket model. Third-stage fins indexed;  $M = 1.82$ .

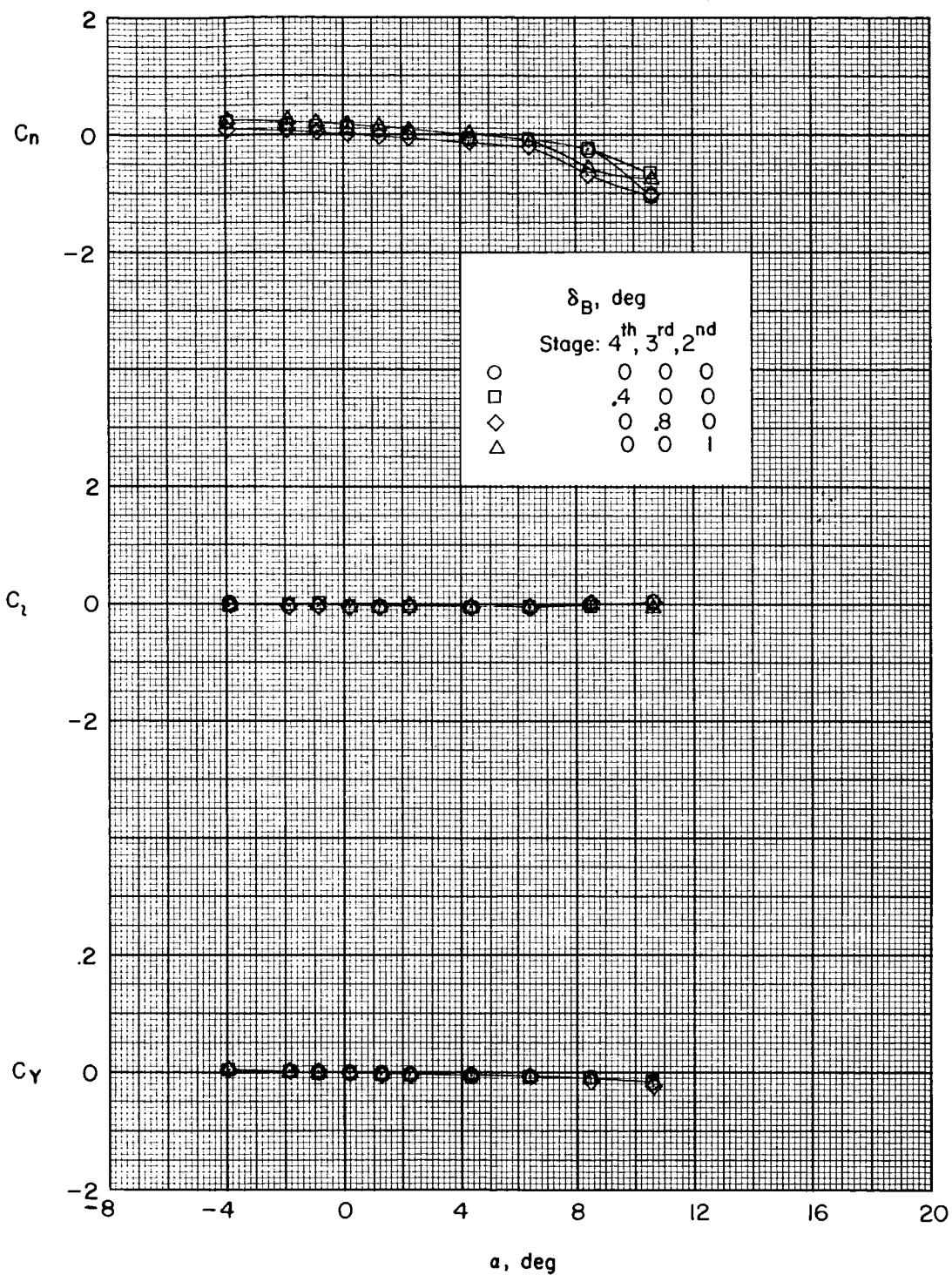


Figure 9.- Concluded.



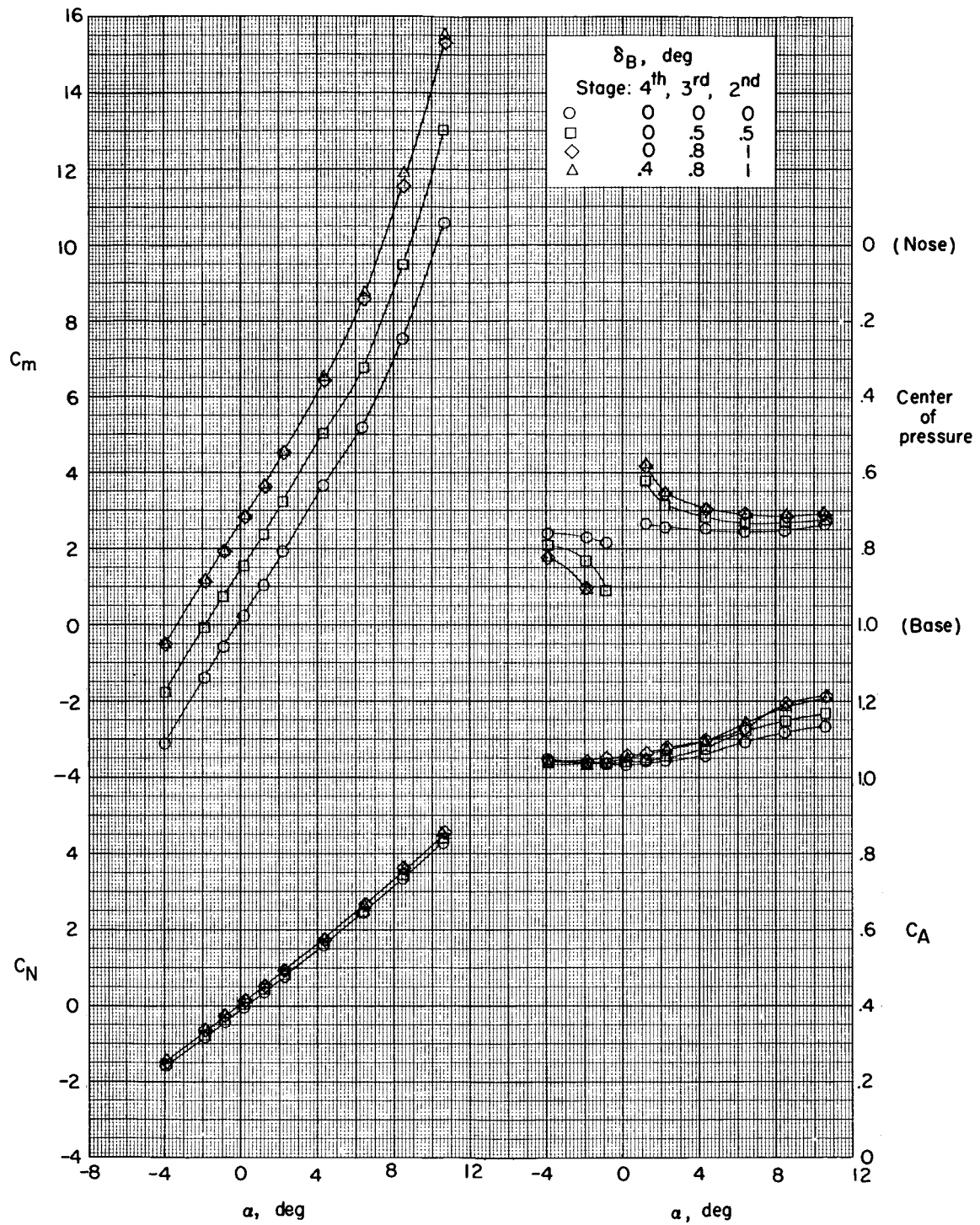


Figure 10.- Effects of combined deflections of various stages of four-stage rocket model. Third-stage fins indexed;  $M = 1.82$ .

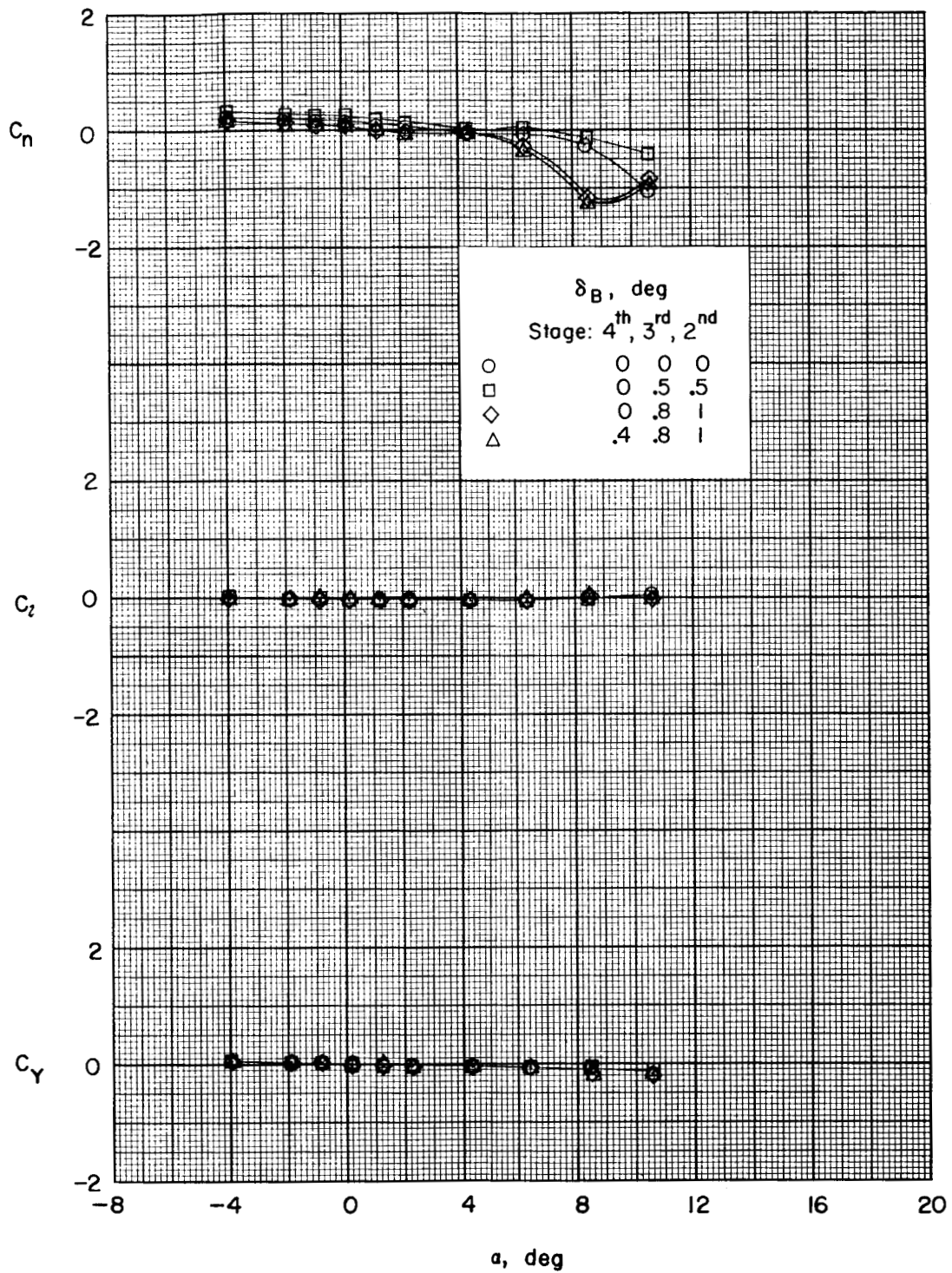


Figure 10.- Concluded.



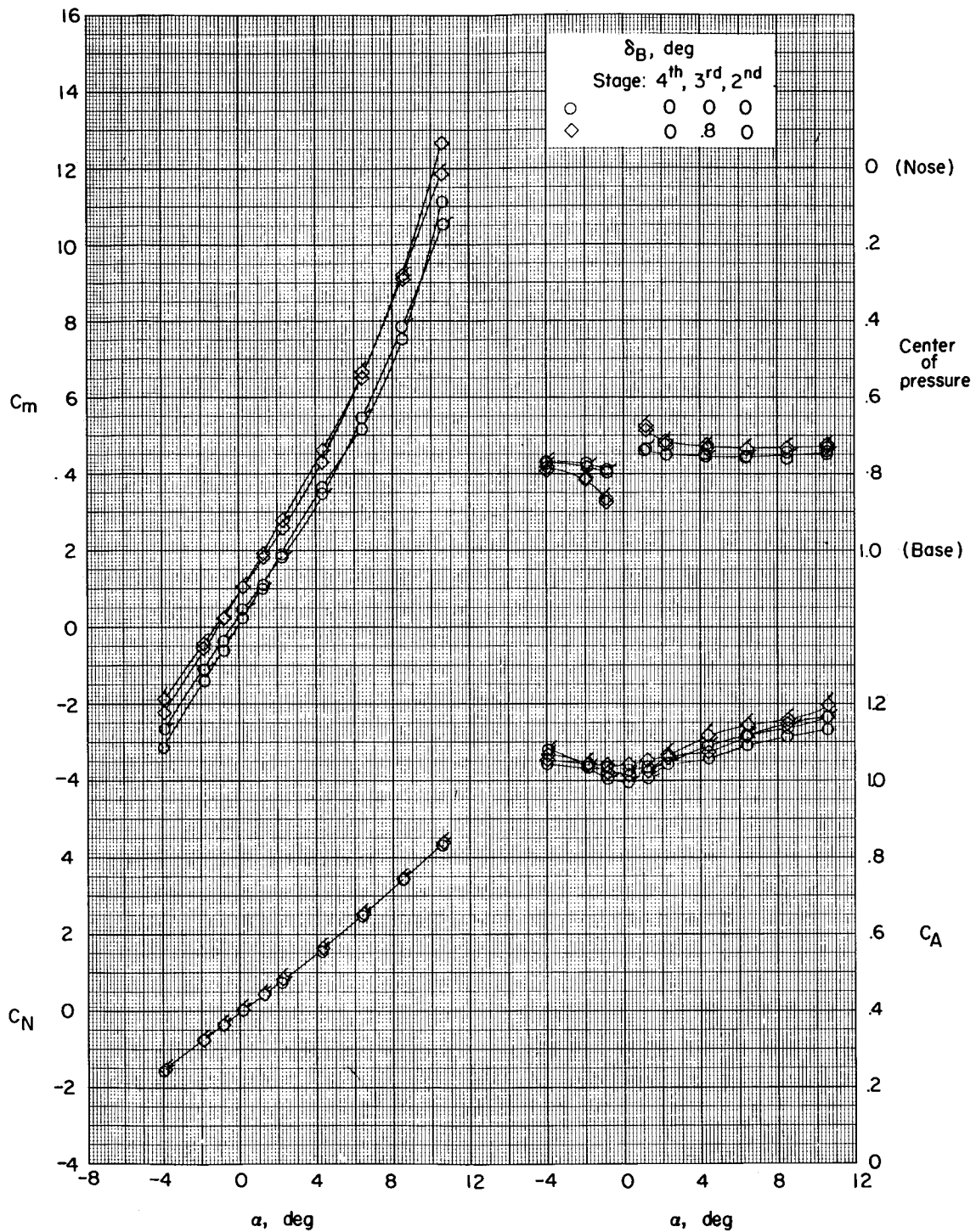


Figure 11.- Effects of third-stage-fin alignment. Plain symbols indicate indexed fins; flagged symbols indicate aligned fins;  $M = 1.82$ .

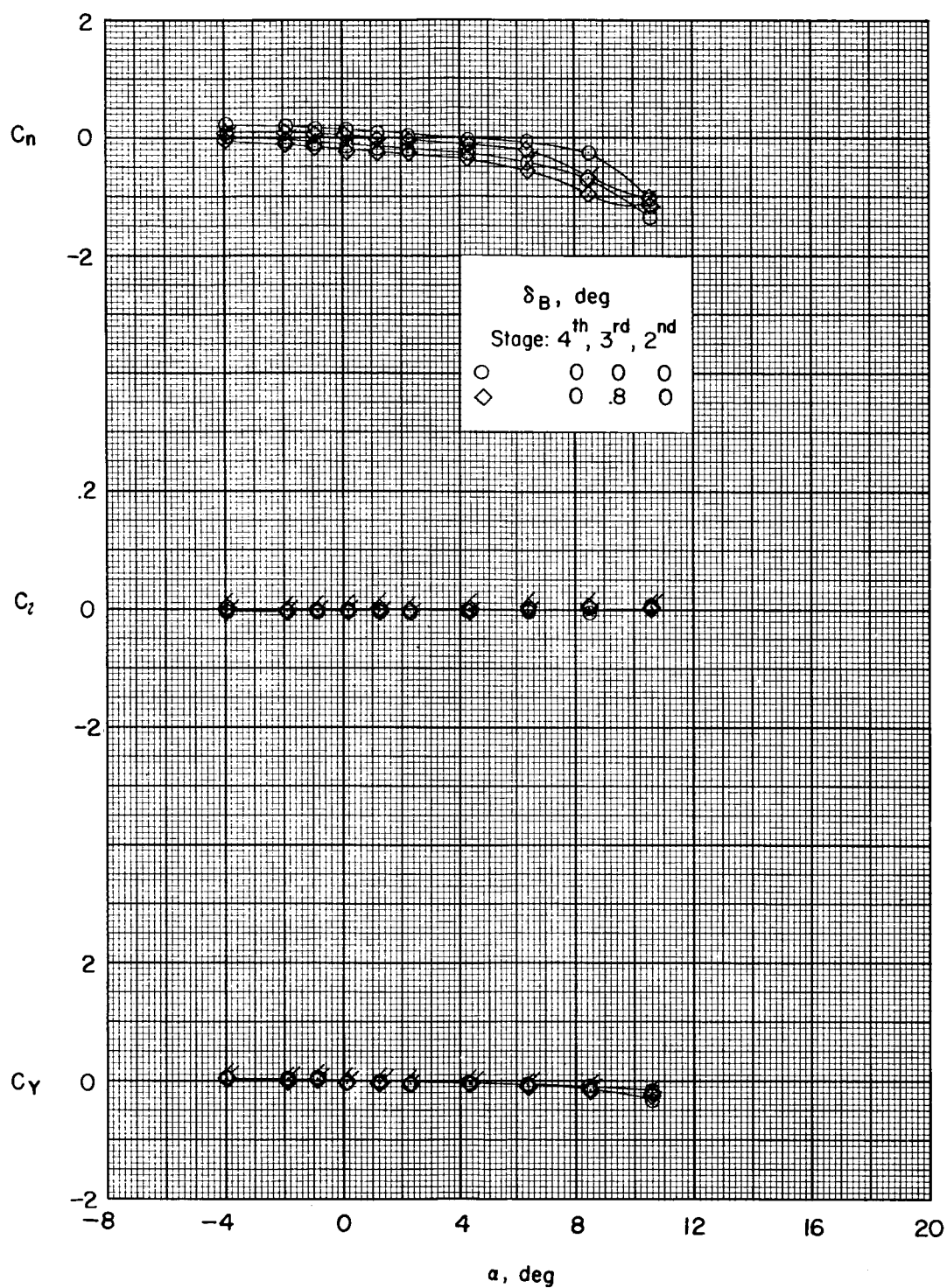


Figure 11.- Concluded.

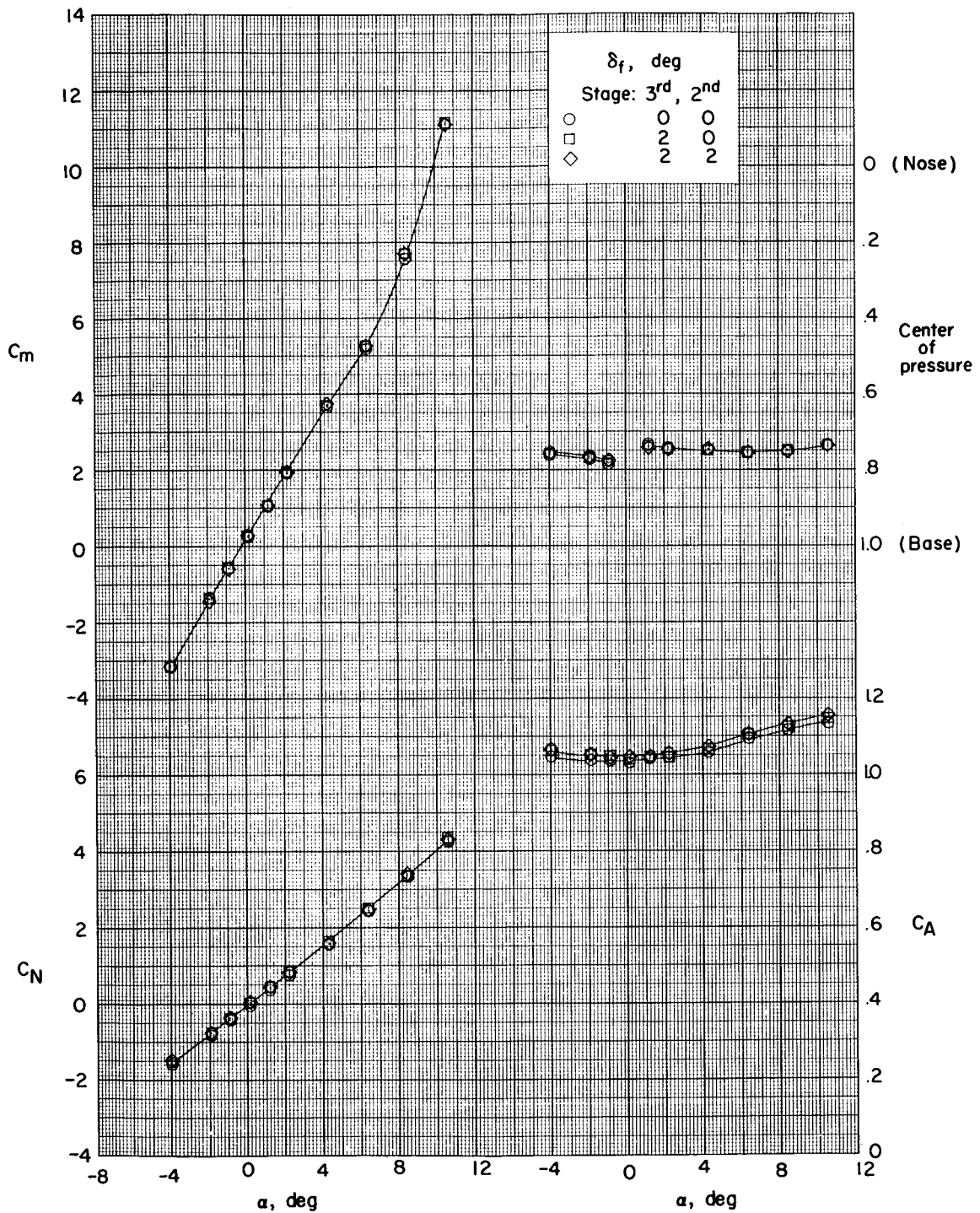


Figure 12.- Effects of differential fin deflection. Body deflection,  $0^\circ$ ; third-stage fins indexed;  $M = 1.82$ .

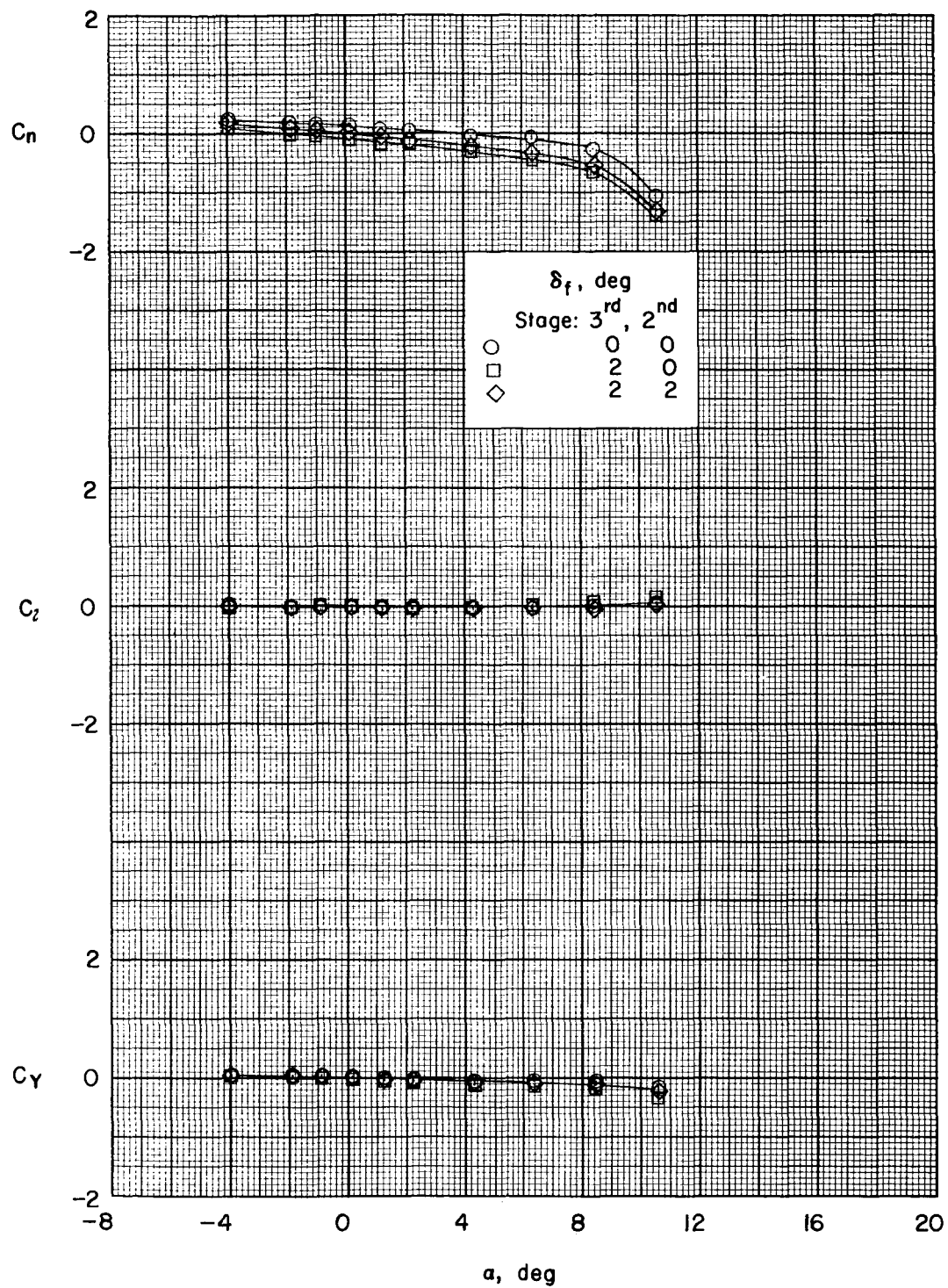


Figure 12.- Concluded.

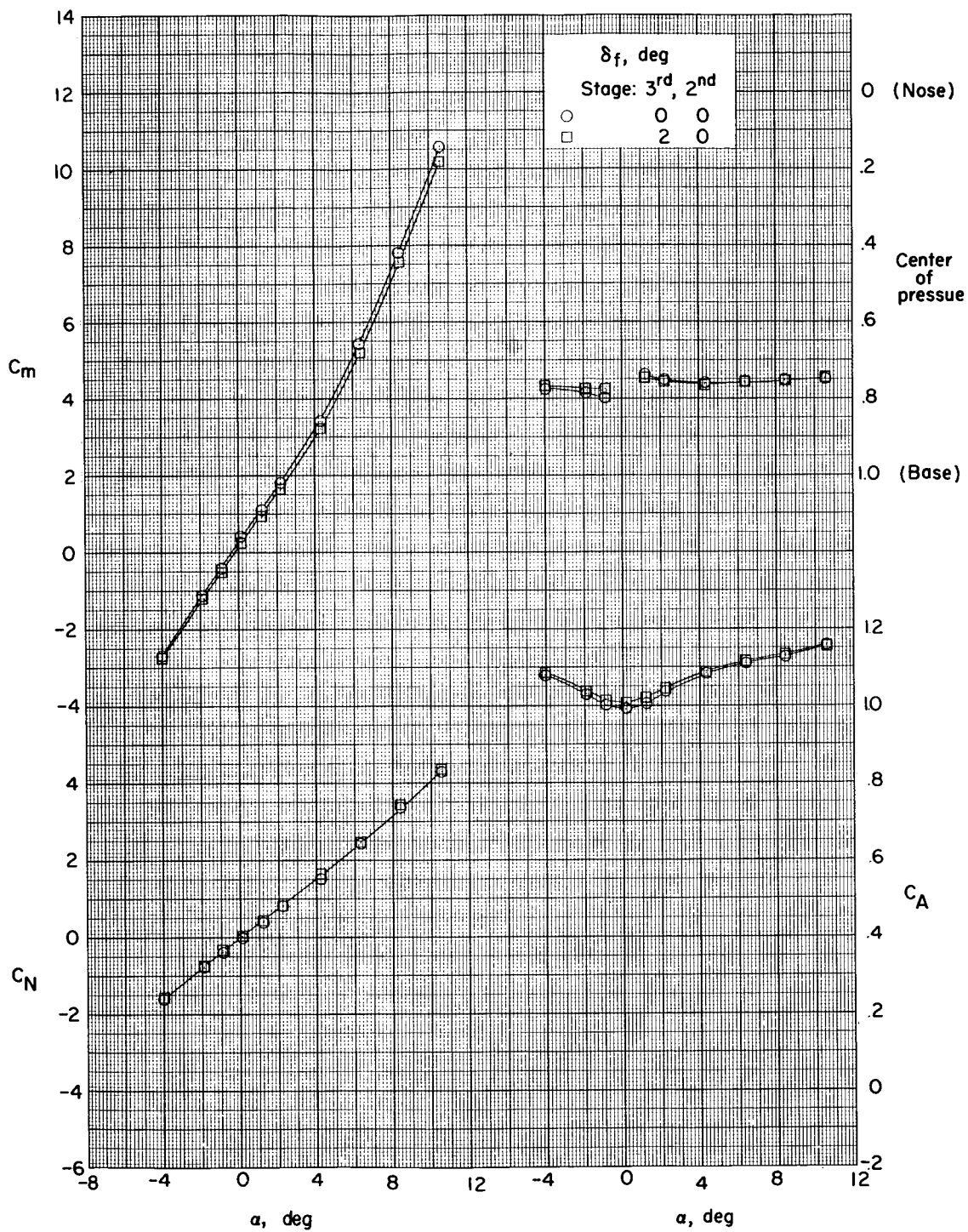


Figure 13.- Effects of differential fin deflection. Body deflection,  $0^\circ$ ; third-stage fins alined;  $M = 1.82$ .

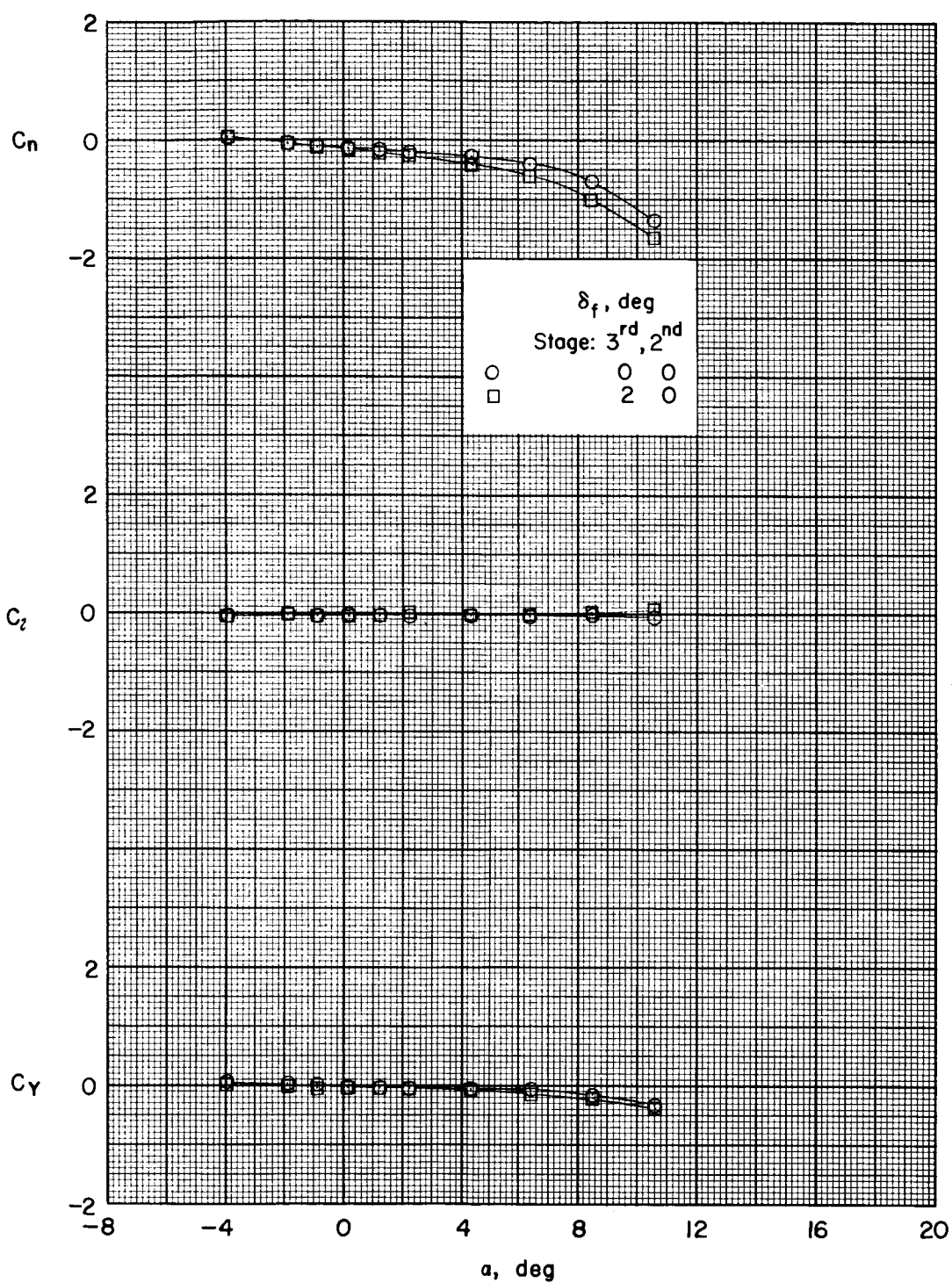


Figure 13.- Concluded.